A Calorimetric, NMR and X-Ray Diffraction Study of the Melting Behavior of Tripalmitin and Tristearin and their Mixing Behavior with Triolein

I.T. NORTON*, C.D. LEE-TUFFNELL, S. ABLETT and S.M. BOCIEK, Unilever Research, Colworth House, Sharnbrook, Bedfordshire MK44 1LQ, England

ABSTRACT

X-ray diffraction, differential scanning calorimetry and NMR have been used to give information on the molecular order and melting of tripalmitin and tristearin crystals. They also have been used to study the melting and solubility of these pure triglycerides when mixed with triolein. From these studies we propose demixing in the liquid state and observe modification of the crystallization kinetics of these saturated triglycerides such that the highest melting (β-polymorphic) form is observed within a minute at 298K for cooling rates up to 120K/min. In the mixtures the long d-spacing, corresponding to the distance between layers in the crystals, was observed to be approximately 0.5 nm greater after cooling in excess of 60K per min than for close packed layers in the β form crystals. A study carried out after rapid cooling showed that two processes occurred. Initially, the α polymorphic form is produced; this transformed to the β-like crystals in a matter of a few minutes. There is then a much more gradual decrease in the long d-spacing as a slow annealing into the tightly packed β polymorphic form occurs.

INTRODUCTION

A detailed understanding of the thermodynamics and mechanism of crystallization of triglycerides has been of interest for some years. In 1934 it was reported (1) that the apparent multiple melting of triglycerides was due to the polymorphic nature of these systems. Since this early work, the number and type of crystalline forms (2) as well as the mechanism of transformation from one type to another (3) have become controversial issues. It is now generally accepted that saturated monoacid triglycerides can form three crystal types, the α-form being the lowest melting, the β'-forms being intermediate and the β-form the most stable polymorph. Although these crystal forms exhibit distinct X-ray patterns and have characteristic physical properties (4,5), the β polymorph is the only form for which it is generally accepted that a molecular structure (6) is known. Although the controversy seems to have been resolved to some extent, two recent papers (7,8) suggest from calorimetric measurements that more than one β'-form can be produced for the two most extensively studied systems, tripalmitin and tristearin. In order to obtain these, however, specific tempering processes were required.

Although a large amount of work has been carried out on individual monoacid triglycerides, little work has been directed at the polymorphic forms produced from binary systems, especially when the melting points of the components are opposite sides of ambient temperature. These are, however, the conditions of greatest interest for many industrial processes. In the past when such systems have been studied, it was to obtain information on solubilities (9,10,11), and because of the high temperature scan rates used (9) at conditions far removed from equilibrium. As there have been a number of advances in physical techniques, it is now possible to study these mixtures in more detail.

The new generation of precision microcalorimeters (12) are 2 to 3 orders of magnitude more sensitive than the best available (13,14) only a few years ago. The use of such a calorimeter allows dilute solutions to be studied and gives good quality results at scan rates as low as 0.2 K/hr. Now it is also possible to study the high resolution nuclear magnetic resonance spectrum of solids (15,16). Although this technique is particularly suited to systems in which long range regular order exists, no previous work has been reported on the polymorphic forms of the triglycerides. We have shown that it is possible to gain information on the environments of particular parts of the molecule in the different polymorphic forms from the chemical shift values of the individual carbon atoms.

These plus a number of other physical techniques were used to study tripalmitin and tristearin and binary systems of either tripalmitin or tristearin in triolein. The evidence obtained suggests that either α or β polymorphic forms can be produced in the pure saturated triglycerides on changing the cooling rate as published previously (17,18). In contrast, when triolein is present only the higher melting point polymorphic form is observed within a few minutes. Ideal mixing of tripalmitin or tristearin with triolein has been reported (10,11) in the past, but our measurements, using the more sensitive physical techniques, show that the saturated triglyceride is less soluble in triolein than predicted.

MATERIALS AND METHODS

The samples of the purified mono-acid triglycerides were supplied by A.P.J. Mank of URL Vlaardingen. The purity was checked by NMR, carbon number gas chromatography and high pressure liquid chromatography (HPLC) of the fatty acid methyl ester (FAME). The tripalmitin was >98% pure and the tristearin was >96% pure. The triolein was analyzed by the above methods, and the *trans* unsaturated content analyzed by silver complexation chromatography; the purity was >97%.

Mixtures were prepared, unless otherwise stated, by heating tripalmitin or tristearin with triolein to 360K and holding there for 10 to 30 min. Rapid cooling generally was achieved by removing the sample from the water bath and plunging into an environment at approximately 260K. A thermocouple within the sample recorded a cooling rate in excess of 60K per min. The sample was then removed from this environment and measurements made at constant temperature. Slow cooling was found to be more difficult to achieve in practice. Cooling was therefore performed at less than 1K per min to the required temperature. This temperature was maintained and physical measurements were made until constant results were obtained.

Differential Scanning Calorimetry

Calorimetric measurements of the melting behavior of the triglycerides studied were carried out on a Setaram Batch and Flow Biocalorimeter. Removable 1 cm^3 cells were used so that solid samples could be studied. Heating rates between 1 and 0.03 K/min were used. The temperature control of the instrument is better than $\pm 5 \times 10^{-3}$ K. Different weight samples were scanned, on both heating and cooling, between 3 and 10 times each against a liquid oil reference. Data were collected by an on line processor (HP85) at a rate of 20 data points per degree. The multiple scans were averaged and a standard baseline (obtained for empty cells) subtracted. Integration was performed digitally

*To whom correspondence should be addressed.

with the heat capacity offset determined by linear least squares fitting of more than 200 data points above and below the peak. Error limits were determined by integration and comparison of individual scans. Both the temperature profile and enthalpy change proved to be very reproducible.

X-ray Diffraction

X-ray measurements were carried out in two ways, both using a Philips Constant potential generator, producing CuK_α radiation ($\lambda = 0.154$ nm), and an Anton Paar TTK camera. In the wide angle range, $1^\circ < 2\theta < 35^\circ$, diffraction was measured with a proportional counter. Temperature control of the sample (dimension 14 mm × 10 mm × 1 mm) was by a Haake F3/K circulating bath with the temperature of the sample monitored by a thermocouple. The angular range was scanned at a rate of 1 deg/min. The small angle range ($0.5^\circ < 2\theta < 8^\circ$) was studied on the above apparatus but was measured using a Kratky camera. The sample dimensions were 8 cm length by 1 mm diameter contained in a thin walled (0.01 mm) glass capillary. In this case scattering was detected by a sealed CGR position sensitive proportional counter.

Nuclear Magnetic Resonance

A very sensitive probe for molecular environment and mobility is nuclear magnetic resonance. There are two distinctly different modes of operation. Broadline (pulse) techniques normally are used to give information on the motions of molecules from the spin-spin (T_2) and spin-lattice (T_1) relaxation times, and so are ideally suited for studying different phases of the same molecule. The use of high resolution NMR allows the study of chemically different sites within a molecule and so can give information about changes in molecular structures. Until recently, high resolution techniques have been confined to the study of liquid or solution states. However, it is now possible to obtain ^{13}C high resolution spectra of solids by the technique known as "cross polarization magic angle spinning" (CP/MAS).

High resolution ^{13}C NMR experiments were carried out on a Bruker CXP-300 spectrometer at a field strength of 7.05 Tesla. A standard Bruker probehead with an 'Andrews' rotor (containing 0.3 g of sample) made of perdeuterated polymethyl-methacrylate was used for the CP/MAS experiments (15,16). Spectra were referenced to the residual signal from the rotor (44 ppm) measured relative to TMS (tetramethylsilane). Experimental conditions were: single contact (5 ms), a rotational frequency of ∿3.8 KHz, 50 kHz spin-locking and decoupling fields and a spectral width of 30 kHz. The temperature was ambient while the acquisition time was 35 ms with a recycle delay of 20 sec (i.e. 3 to 4 times the proton T_1 of the solid). Between 200 and 1000 scans were averaged.

The liquid state spectrum was obtained with a standard high resolution probehead (10 mm sample tube) at 353K. Broad-band gated decoupling was used to suppress the nuclear overhauser effect. Purity checks by NMR were carried out in $CDCl_3$ solutions and were based on the method of Pfeffer (19).

Proton relaxation time data was obtained using a Bruker CXP series pulse spectrometer operating at a frequency of 60 MHz, equipped with a 10 mm variable temperature probe. In order to avoid sample contamination or interference caused by the introduction of a temperature sensor, the probe temperature calibration was obtained separately using a thermocouple in a sample of olive oil. The Free Induction Decay signal was recorded on a Datalab DL905 transient recorder in the dual time-base mode interfaced to the spectrometer Aspect 2000 computer. This allowed the very rapid decay from the solid phase to be acquired together with the much slower decay from the liquid phase. T_1 relaxation times were measured using the 180°-τ-90° pulse sequence (20), with the FID following the 90° pulse acquired for each τ delay value used.

RESULTS AND DISCUSSION

Single Component Systems

Calorimetric measurements. The melting behavior of tripalmitin and tristearin have been studied, as a function of scan rate, using the calorimetric method. Within the range of rates used (1-0.05 K/min), there are changes in the shape of the heat capacity temperature profile, as shown in Figures 1 and 2. On reheating tripalmitin which had been crystallized from the melt cooled at a rate of 0.5 K/min, an exotherm at ∿320K was followed by an endotherm at ∿340K (Fig. 1). However, if crystallization was from a melt cooled at 0.125 K/min, the exotherm was no longer present and only the endotherm (peak maximum 339.7K) was observed (Fig. 1). Scanning at lower rates produced a curve identical to that observed at 0.125 K/min, suggesting that the equilibrium is closely approached at scan rates lower than 0.1 K/min.

Scan rate dependence is expected from classical thinking (21) on melting curves from DSC equipment, where the melting point is calculated by extrapolating the leading edge of the peak to the point where it meets the baseline (22). However, the lack of scan rate dependence suggests that the peak maximum should be taken as the melting point from the new precision calorimeters, bringing this method into line with visual methods. The width of the peaks for both tripalmitin and tristearin can be explained

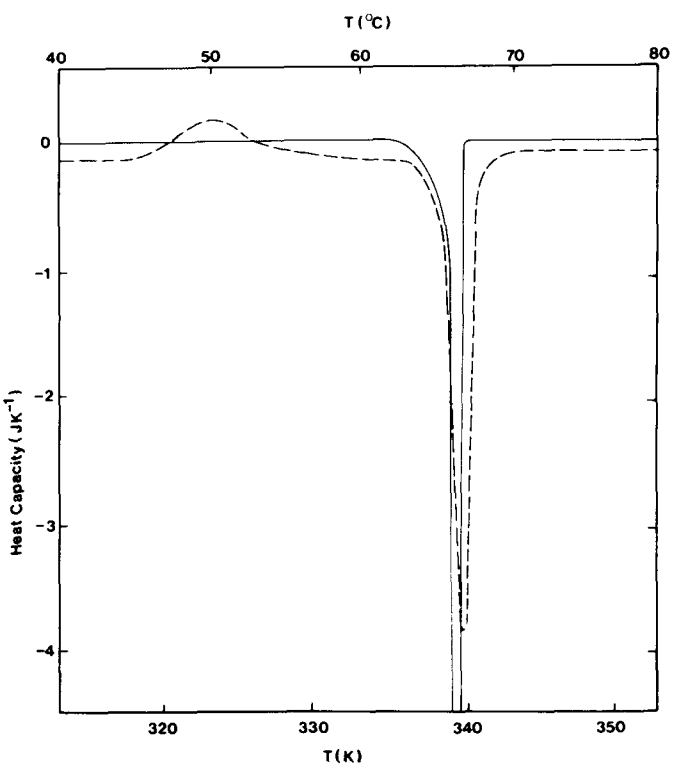

FIG. 1. Heat capacity temperature profiles for the heating of pure tripalmitin (32 mg) obtained on temperature cycling at 0.5 K/min (---) and 0.125 K/min (——) between 280 and 360K. The heat capacity scale for the slower scan has been drawn to demonstrate the lack of an α to β exotherm.

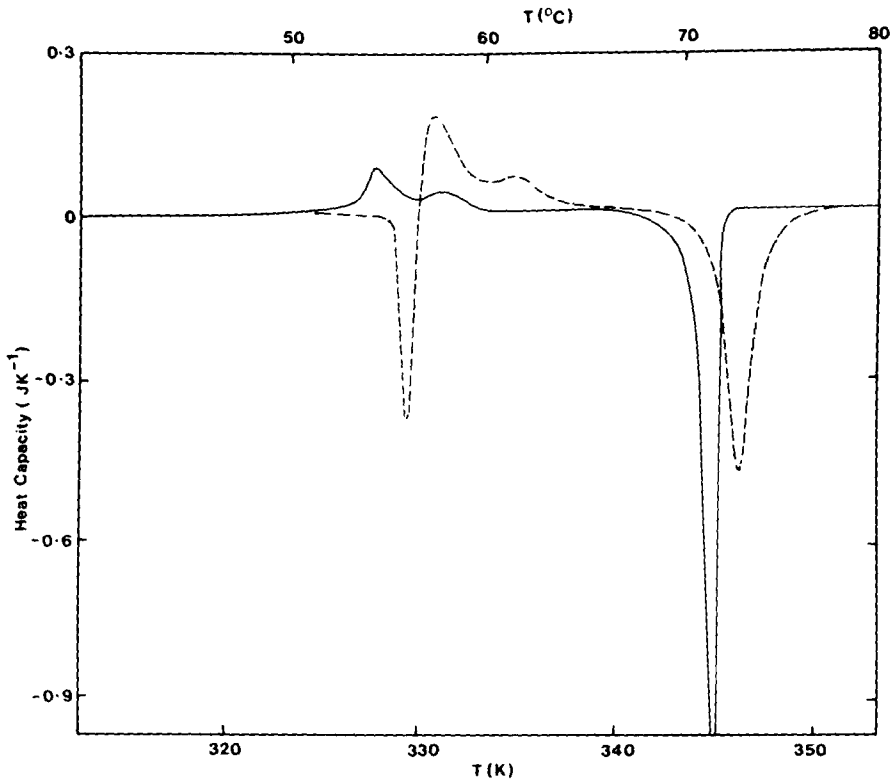

FIG. 2. Heat capacity temperature profiles obtained for the heating of pure tristearin (4.4 mg) on temperature cycling at 1 K/min (----) and 0.1 K/min (——) between 280 and 360K.

in terms of the impurity levels in these materials. The melting temperature determined by this method for tripalmitin is 339.7K, which compares favorably with the previously reported (8,13,14,18) values for the β melting temperature 339.6K (66.4 C). Integration of the endothermic peak gives the enthalpy change as 170 ± 1 kJmol^{-1}, which is in agreement with the previously reported data (8,13,14,18,23), i.e. an average of 172 ± 6 kJmol^{-1}.

X-ray powder diffraction patterns were obtained in order to assign the peaks to particular polymorphic transitions and to check that on slow cooling only the most stable polymorphic form was produced. The slow cooled sample from the DSC measurement gave a typical β-spectrum (18,24) with intense diffraction peaks corresponding to the three major d-spacings, 0.372, 0.390 and 4.465 nm. On cooling at 0.5 k/min or faster only a single strong diffraction peak at 0.419 nm was observed, which is diagnostic of α-type crystals (18,24). Samples which were heated above the exotherm (i.e. 328K) and then restudied at 298K also gave the β-diffraction pattern.

The evidence from the X-ray study gives us confidence in assigning the exotherm to an α to β polymorphic transformation even though it is some 2K higher than previously reported. Calculating the enthalpy change for α melting as the difference between the endothermic and exothermic peaks gives ΔH_f = 143 ± 3 kJmol^{-1}. The value obtained from the cooling curve where only a single exothermic peak was observed at ∿318K (the melt to α polymorphic form transition) was ΔH = 130 ± 5 kJmol^{-1}. These are similar to the values reported for the α melting in references 14 and 18 (i.e. 127 ± 6 kJmol^{-1}), but somewhat different from the value reported in (8), 103 kJmol^{-1}.

DSC studies carried out on tristearin revealed closely similar results. One major difference is that when crystallization was from a sample cooled at a rate between 0.5 and 1 K/min, on reheating at 0.5 or 1 K/min we observed what looked like the start of a melting endotherm at 326K, which was followed by an exotherm (Fig. 2). The shape of this curve in fact suggests that the α-form crystals had undergone a significant amount of melting before the rate of β crystallization releases enough energy to reveal the exothermic peak. This explanation is supported by the position of the peak which agrees with the literature value (10,14,18) for α melting. In addition, on reheating at slower rates the initial endothermic peak is no longer observed with the curve being very similar to that observed for the more slowly cooled sample (Fig. 2).

On reheating tristearin which had been crystallized at 0.1 K/min the exothermic peak at ∿326K was still observed (Fig. 2). This can now be seen quite clearly as a doublet with the peak maxima being 327.5 and 330.2K. The origin of this doublet peak is still uncertain, as we have been unable to obtain any evidence of β' crystals from X-ray studies although such an explanation of the doublet peak is unlikely as the β' to β transformations are reported as occurring at higher temperatures 334 and 337K (7,18).

The position and shape of the endothermic peak were again independent of scan rate below 0.1 K/min. Integration of the peak at 345.5K (i.e. the β to melt transition) gave ΔH = 190 ± 5 kJmol^{-1}. The melting point and enthalpy change are very similar to the previously reported values (10,13,18,23); i.e. 345.3K (73.1 C) and an average ΔH = 196 ± 7 kJmol^{-1}. The difference between the endothermic and exothermic peaks gives ΔH = 144 ± 3 kJmol^{-1}, which is in close agreement with the value found for the exothermic peak at 326K on cooling for the melt to α form crystallization, 137 ± 5 kJmol^{-1}. Our values for this transition are the same as those reported in (14) and (18), i.e. an average of 145 ± 5 kJmol^{-1}, but are again somewhat larger than the value obtained by Hagemann and Rothfus (8), ∿113 kJ and mol^{-1}.

NMR measurements. We have used both forms of NMR

TABLE I

Spin-lattice (T_1) Relaxation Times for Tristearin and Tripalmitin in the α and β Crystal Forms

Triglyceride	α crystal form	β crystal form
Tristearin	0.38 sec	2.8 sec
Tripalmitin	0.46 sec	5.4 sec

described earlier to study the different polymorphic forms of tripalmitin and tristearin. As the general rule is that the T_1 relaxation time for solids is directly related to the molecular motion, our pulse measurements show (Table I) that the α form of the triglycerides has an apparent greater degree of motional freedom. However, as overall relaxation can occur through, and therefore be dominated by, the most mobile region, i.e. by spin diffusion, it is possible that the shorter T_1 value for the α form is due to a specific site in the molecule (e.g. methyl groups). A detailed analysis of the molecular motion of specific sites will be the subject of a subsequent publication.

Although the resolution of the CP/MAS spectra of the solid triglyceride is not as good as that obtained from the same sample in the liquid state (Fig. 3), there are obvious similarities between the spectra which allow the peaks observed for the solid to be assigned to particular carbon atoms within the molecule. The ^{13}C spectra obtained for the α and β polymorphic forms of the tripalmitin (Fig. 3) show significant and reproducible differences. The peaks corresponding to the carbons of the terminal methyl group (14-16 ppm) and the glycerol group (60-70 ppm) have different chemical shifts for the two forms, suggesting a change of environment for these regions of the chain. Also in the β-form the 1 and 3 positions of the glycerol group are resolved so that the two carbons are no longer equivalent. Both these observations are consistent with the proposed models for the two types of crystal structure with the change of form resulting in the rearrangement of the glycerol group, and the α-form containing two fatty acid chains in identical conformations. The observation for the α-form that the carbons next to the carboxyl group (20-30 ppm) were split into a 2:1 ratio, supports such a model. Almost identical results were obtained for tristearin.

Statistical thermodynamic calculations of internal entropy for the different polymorphic forms. From the NMR measurements it is difficult to see how one of the fatty acid chains can retain its rotational freedom in the α-form as previously reported (8). The molecular models for the different polymorphic forms were, therefore, checked by comparing predicted changes in entropy from statistical thermodynamics with those observed experimentally. The change in internal entropy is given statistically by the partition function over the allowed degenerate states. Therefore, for a hydrocarbon chain with three equally allowed states for each atom in the chain, the change in internal entropy on losing rotational freedom is given by:

$$\Delta S_{int} = R \ln (1/3)^{n-3}$$

where R is the gas constant ($Jmol^{-1}K^{-1}$), $(1/3)^{n-3}$ is the partition function and n is the number of atoms in the chain that lose rotational mobility. The model (6) for the β polymorphic form of saturated mono-acid triglycerides is one in which no internal rotational freedom is retained. Using this approximation the calculated change in internal entropy $\Delta S_{int} = 466\ Jmol^{-1}K^{-1}$ for tripalmitin and 520 $Jmol^{-1}K^{-1}$ for tristearin, which compare favorably with the

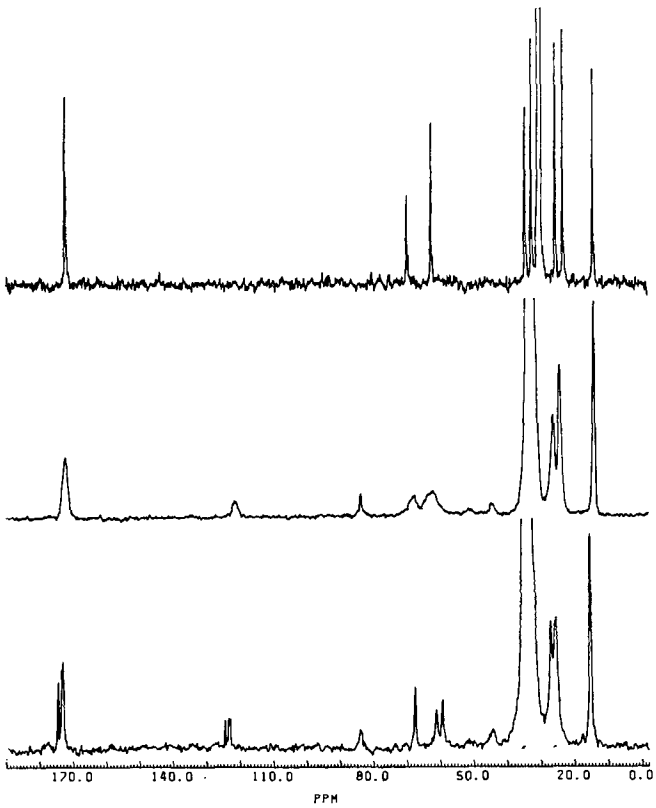

FIG. 3. A comparison of the ^{13}C high resolution spectra obtained for tripalmitin; high temperature liquid spectrum (upper curve), α polymorphic form (middle curve), and the β polymorphic form (lower curve). All three spectra are referenced to external TMS.

experimental results reported previously (8,14,18) and those obtained in this work, i.e. 500 $Jmol^{-1}K^{-1}$ for tripalmitin and 550 $Jmol^{-1}K^{-1}$ for tristearin. The underestimation of approximately 30 $Jmol^{-1}K^{-1}$ may reflect the loss of translational entropy on forming the crystals.

The agreement between the experimental and predicted results suggests that the β form retains little internal motion. In contrast it has been suggested from calorimetry measurements (7,8) that one of the hydrocarbon chains retains its rotational freedom in the α-polymorphic form. This was proposed as the observed entropy change for the α-melting was approximately two-thirds that for the β-melting. In fact our results and a number of those reported previously (14,18) show that for both tripalmitin and tristearin this is not the case, with the observed entropy changes being 80 to 90% of that for the β melting. This suggests that on average 10 to 20% of the molecule retains rotational freedom in the α-form. Therefore, a model in which one chain remains mobile would appear to be unrealistic.

Binary Systems

Equilibrium studies. The precision microcalorimeter was used to obtain the heat capacity as a function of temperature, at a number of scan rates, for mixtures of tripalmitin or tristearin with triolein. The production of the β polymorphic form in these studies was shown by both the X-ray scattering and CP/MAS NMR techniques. A typical DSC scan obtained at 0.2 K/min is shown in Figure 4. The two major features of this curve are as reported previously (9): the absence of an exotherm at low temperature, confirming the X-ray and NMR results that only the β form is produced, and the very wide temperature range of the peak. The transitions were found to be independent of DSC scan

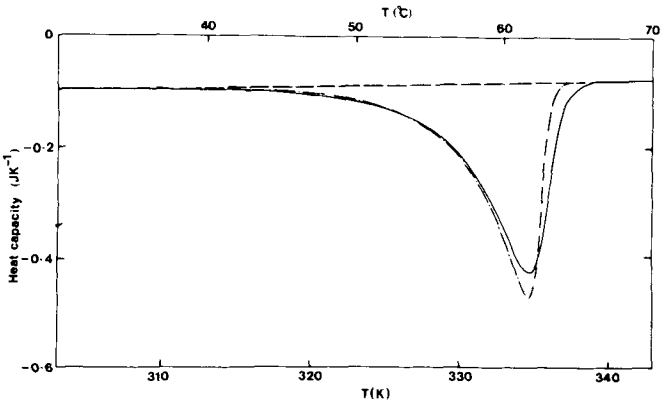

FIG. 4. Heat capacity temperature profiles for a mixture of 43% tripalmitin in triolein (sample weight 24.4 mg) after mixing cold (—•—•—•) and hot (——). Scan rates used were 0.5 K/min for the cold mix and 0.2 K/min for the hot mix.

TABLE II

Enthalpy Data at Various Concentrations for Tripalmitin and Tristearin in Triolein

% PPP	ΔH/kJmol^{-1}	% SSS	ΔH/kJmol^{-1}
100	170 ± 1	100	190 ± 5
69.6	156 ± 4	47	190 ± 2
53.0	159 ± 4	20	180 ± 2
36.3	155 ± 2	2.5	172 ± 4
16.6	154 ± 3	1.1	180 ± 6
3.4	164 ± 2	0.75	190 ± 5
1.0	179 ± 4	0.12	174 ± 10

rate below 0.2 K/min. The peak also is observed to be asymmetric and to have moved to lower temperatures than for the pure material (cf. Fig. 1,4,5,6). As the mole fraction of crystallizing triglyceride is lowered it is quite noticeable that the peak continues to broaden. It also appears that the enthalpy change decreases in the intermediate mole fraction range for mixtures involving tripalmitin but not for those involving tristearin (Table II). No "melting points" were determined for these mixtures, as once the peak becomes so broad it is impossible to obtain a point from the DSC curve which we might call the "melting temperature."

The CXP-60 pulse NMR spectrometer was used to study the amount of crystalline triglyceride present at 303K. This was achieved by comparing the intensity of the slowly decaying portion of the FID signal with the corresponding intensity at 353K, when the tripalmitin or tristearin were in the liquid state. After the intrinsic temperature dependence of the NMR signal and the proton density difference between the saturated triglyceride and the triolein had been allowed for, all of the triolein present was accounted for in the slowly decaying, "liquid-like" portion of the signal. Therefore, there was no evidence of any immobilized triolein. This NMR result suggests that the shift in peak position and width observed by the DSC were not due to mixing of triolein into the tripalmitin crystals. However, small amounts of mixed crystals would not be picked up by this approach (<1%). The lack of mixed crystals was therefore further checked by weighing solid tripalmitin into the DSC cell with triolein added at room temperature. The first scan obtained (Fig. 4) had shifted and broadened to the same extent as those observed when the mixing was carried out at high temperature. This clearly demonstrates that the change in peak shape and position was not due to mixed crystal formation but probably was a result of the solubility of the saturated triglyceride in the liquid oil.

Comparison of observed and theoretically predicted DSC peaks. Considering the accuracy of the DSC technique, both the position and shape of the heat capacity profile can be compared with the values predicted from ideal mixing equations. Comparisons made in this way should prove to be more reliable than trying to obtain a single temperature from the DSC curve. In the mixtures the difference in heat capacity at any temperature over that observed for the pure solid will be due to the heat capacity of the liquid component plus a contribution from dissolving the solid. The contribution to heat capacity from the liquid component is removed by using the liquid as the reference. Any discrepancy in weighing the sample and reference is observed as a simple offset of the total scan, which then can be substracted. The observed peak is therefore due only to the dissolving solid. Using the symbols $C_p(T)$ for the heat capacity at constant pressure of the mixed system and $C_p'(T)$ for the heat capacity of the reference system at temperature T, if ΔH_f is the enthalpy change per mole for the crystallizing material (component 1), the rate of change of liquid phase with temperature is given by:

$$C_p(T) = \Delta H_f \frac{dn_1}{dT} \qquad [1]$$

where n_1 is the number of moles of component 1 that dissolve.

As we are considering only ideal mixing behavior (i.e. ideal solutions) then dissolution DSC curves can be derived by applying simple equilibrium conditions. The mole fraction of component 1 in the liquid phase x_1^l is given by:

$$x_1^l = \frac{n_1^l}{n_1^l + n_2^l} \qquad [2]$$

where n_1^l is the number of moles of component 1 in the liquid phase, and n_2^l is the number of moles of liquid component 2, a constant.

By combining equations [1] and [2] we obtain:

$$C_p'(T) = \frac{n_2\ \Delta H_f}{(1-x_1^l)^2} \frac{dx_1^l}{dT} \qquad [3]$$

For any equilibrium we can describe the equilibrium constant at all temperatures by using the van't Hoff equation:

$$\frac{d\ln K}{d(1/T)} = -\frac{\Delta H_f}{R} \qquad [4]$$

If we consider mole fractions and specific solubility equilibria the Hilderbrand equation applies:

$$\frac{d\ln x_1^l}{d(1/T)} = -\frac{\Delta H_f}{R} \quad \text{or} \quad \frac{dx_1^l}{x_1^l} = \frac{\Delta H_f}{RT^2}\,dT \qquad [5]$$

Integration with the pure substance as the reference state gives:

$$\ln x_1^l = \frac{\Delta H_f}{R}\left(-\frac{1}{T_t} + \frac{1}{T}\right) \qquad [6]$$

where T_t is melting point of a pure crystal. By combining the Hilderbrand equation [5] and equation [3], we obtain:

$$C_p'(T) = \frac{n_2\ (\Delta H_f)^2}{RT^2} \frac{x_1^l}{(1-x_1^l)^2} \qquad [7]$$

Thus, equation [7] allows the heat capacity, at any temperature and any liquid mole fraction of component 1, to be predicted. However, equation [6] allows the calculation of the solubility of component 1 at any temperature and therefore the mole fraction in the liquid state. By using both equation [6] and [7], therefore, it is possible to predict heat capacity curves for any ideally mixed system, provided that the enthalpy change and melting temperature of the pure system are known. $C_p(T)$ curves were generated for idealized mixtures, with the thermodynamic parameters

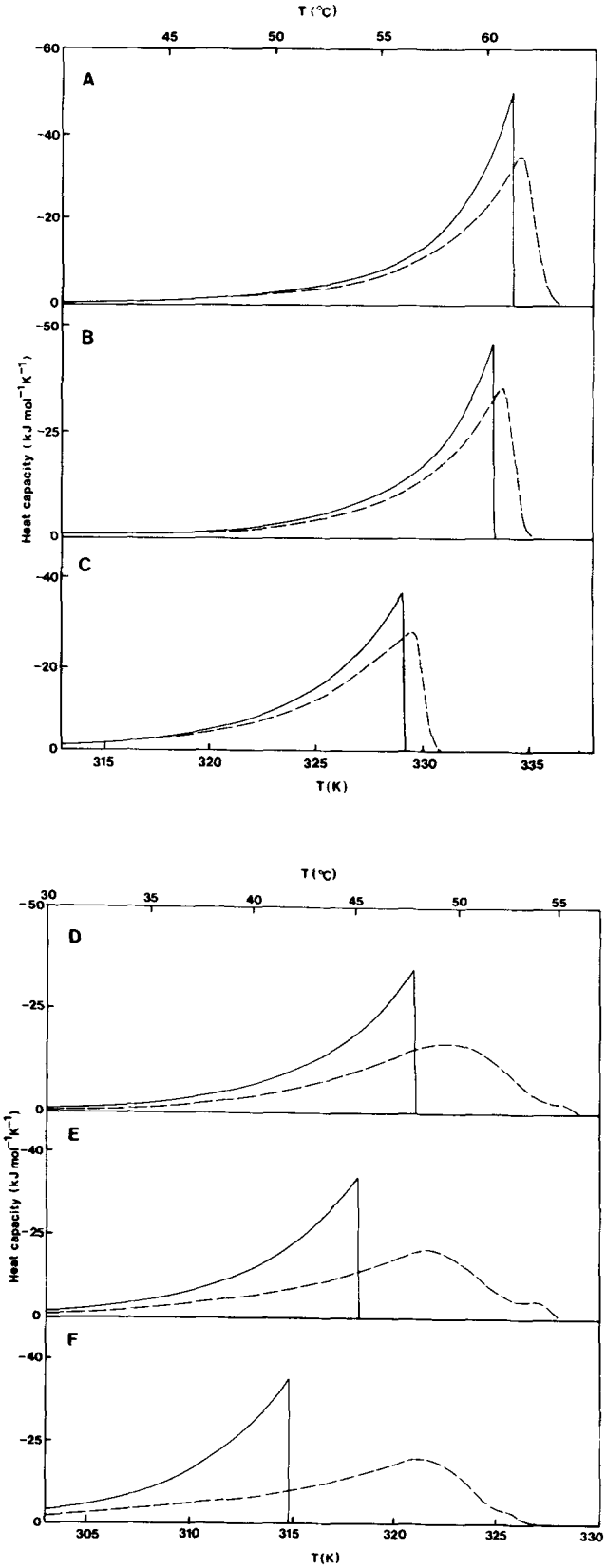

FIG. 5. Comparison of the observed (---) and theoretically predicted (——) heat capacity temperature profiles for mixtures of tripalmitin and triolein. Tripalmitin mole fractions of 0.39 (curve A), 0.33 (curve B), 0.15 (curve C), 0.031 (curve D), 0.018 (curve E) and 0.009 (curve F). The observed data was collected at a number of scan rates between 0.05 and 0.2 K/min for each sample.

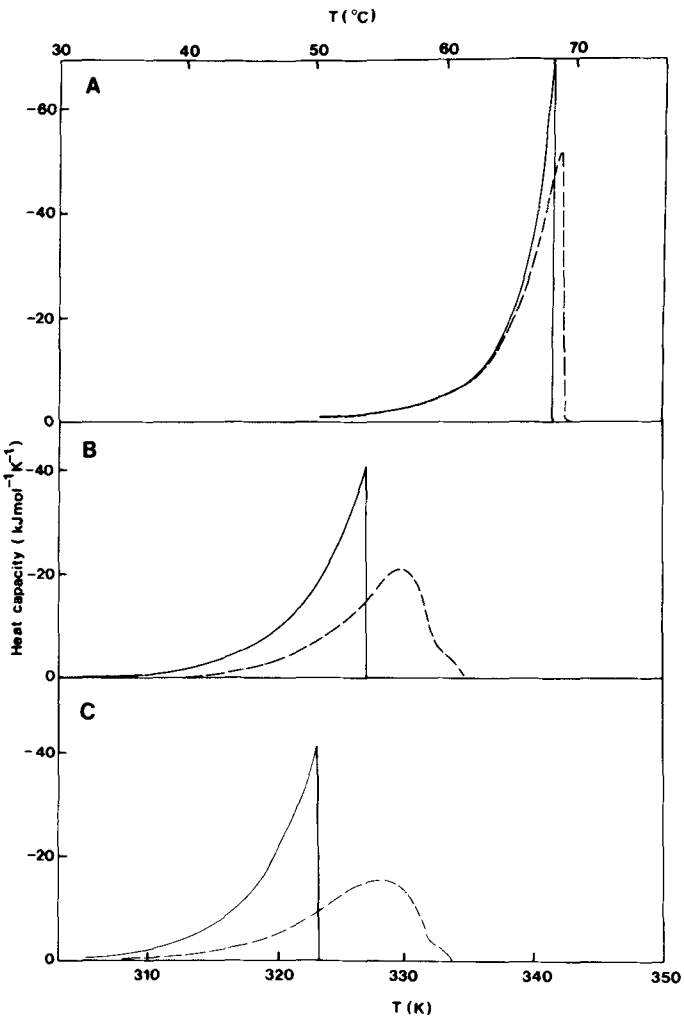

FIG. 6. Comparison of the observed (---) and theoretically predicted (——) heat capacity temperature profiles for mixtures of tristearin and triolein. Tristearin mole fractions of 0.47 (curve A), 0.025 (curve B) and 0.011 (curve C). Observed heating curves were obtained at a scan rate of 6 K/hr.

taken from the study of tripalmitin and tristearin described above. Comparisons were made for the conditions of 1 mole of solute in the mixture and are shown in Figures 5 and 6.

Theoretical and observed $C_p(T)$ curves for tripalmitin are compared in Figure 5. Although the agreement between the observed and theoretical curves is fairly good, in the mole fraction range of 0.40 to 0.15, there appears to be a systematic deviation with the experimentally observed peaks being broader and at higher temperature than predicted. This phenomenon is more clearly demonstrated at lower concentrations (Fig. 5), where dramatic differences in temperature profiles of the peaks are observed. The same general trend was observed for tristearin (Fig. 6). The occurrence of the peaks at higher temperature than predicted shows that the saturated triglyceride is less soluble in the triolein than predicted.

Solubility of the saturated triglycerides in triolein. These results cannot be explained in terms of impurities, as any deviation resulting from impure materials would tend to lower the melting temperature and make the saturated triglyceride appear to be more soluble than predicted. In addition, although the melting temperature could be higher considering the fact that the saturated triglycerides are only 97-98% pure, this would make less than 0.5K difference in

the peak maxima. This may account for a substantial amount of the discrepancy at higher mole fractions, but obviously makes an insignificant difference at the lower concentrations, where the temperature difference is greater than 5K. We would predict from these measurements that demixing in the solution state is occurring with the solubility of the crystallizing triglyceride below that expected.

In order to support the calorimetric measurements, X-ray diffraction and pulse NMR were used to obtain the percentage solid tripalmitin as a function of temperature for the mixed systems. The results obtained were in agreement with the calorimetric measurements, although the low mole fractions of crystallizing material were not studied because of the low sensitivity of these instrumental techniques. We are presently in the process of developing novel NMR and infrared methods to study low levels of solids in the presence of excess liquid. For the low concentration we have used light microscopy to give qualitative information on melting profiles. These studies show that substantial amounts of crystalline material exist at temperatures above the predicted end points from ideal mixing equations and remain at temperatures similar to those observed as the end point from calorimetric measurements.

Although the cause of the demixing in the liquid state is not clear it might be suggested that, because of the steric nature of the *cis* unsaturated bond in the triolein, rotation about the carbon-carbon bonds next to this region causes exclusion of other molecules. As the structure of the saturated molecules are more compatible with each other it does not seem unreasonable that they remain together in the liquid state.

Non-equilibrium studies. In order to understand the mechanism of crystallization in the binary systems, we crystallized the saturated triglyceride under distinctly different cooling conditions, as described in the materials and methods section.

At 298K, X-ray diffraction measurements carried out on both tripalmitin and tristearin at various concentrations in triolein showed only the β diffraction pattern for all cooling rates studied. In the low angle region, however, the d-spacing corresponding to crystal layers was found to be greater immediately after rapid cooling. The diffraction peak corresponding to this d-spacing also was observed to decrease in intensity and become 2-3 times broader, showing that the distances between layers are not only greater than for the β polymorphic form, but also less well defined. Similarly, the CP/MAS NMR revealed a 'β like' spectrum, but the slow and rapid cooled samples had different chemical shift values for the methyl and glycerol carbons. The values obtained for the slow cooled sample were the same as those obtained for the slow cooled pure triglycerides. It also was observed that the spectra obtained on the rapid cooled samples had peaks due to carbons from the triolein. This evidence might suggest that triolein had been incorporated into tripalmitin crystals, but this clearly is not correct as we have shown that the liquid like component of the free induction decay NMR signal accounts for all of the triolein present. The most likely interpretation of these results is that the triolein is in a liquid state and the presence of triglyceride crystals causes the triolein molecules to exhibit anisotropic motion which allows it to contribute to the solid state spectrum. It was found that the Hartmann-Hahn matching conditions (25) required to observe the triolein peaks were much more critical than those for the solid triglyceride, and this is in complete agreement with the above proposed model. Similar results and conclusions have been reported recently for a NMR study of seeds, where the liquid lipid component of the seed was shown to contribute to the CP/MAS spectrum (26).

Calorimetric measurements on the rapid cooled samples show different heat capacity profiles from those obtained for the equilibrium studies (Fig. 7). The heat capacity of the rapid cooled sample is approximately 300 $Jmol^{-1}K^{-1}$ greater at 310K than the slow scanned (equilibrium) studies. This suggests that there is more freedom (randomness) in the rapid cooled sample, thus requiring more energy to raise the temperature. Proton relaxation results are consistent with this observation as reflected in the T_1 value for the solid component of the free induction decay, 2.2 secs for the rapid cooled sample and 4.7 secs for the slower cooled sample. These results could be explained by the model proposed above, with the smaller crystals produced on rapid cooling causing the increased disorder.

Figure 7 shows the difference in the DSC peak shape for the repeated slow scans (0.5 K/min) and the first scan after cooling in excess of 60 K/min. As can be seen, although the heat capacity at low temperature is greater for the rapid cooled sample, the peak starts at higher temperature and, as the maximum of each trace is at the same temperature, it is sharper. Integration of the peaks reveals that

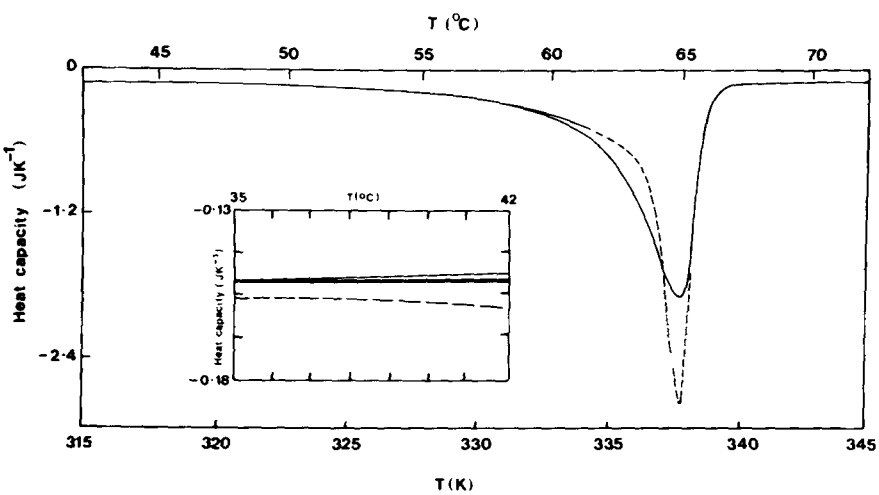

FIG. 7. Heat capacity temperature profiles for a mixture of 70% tripalmitin in triolein. All scans were obtained at a heating rate of 0.5 K/min. Three duplicate heating scans on the same sample after cooling at 0.5 K/min are shown (——) and after cooling in excess of 60 K/min (---). An expansion of the heat capacity axis is shown in the insert.

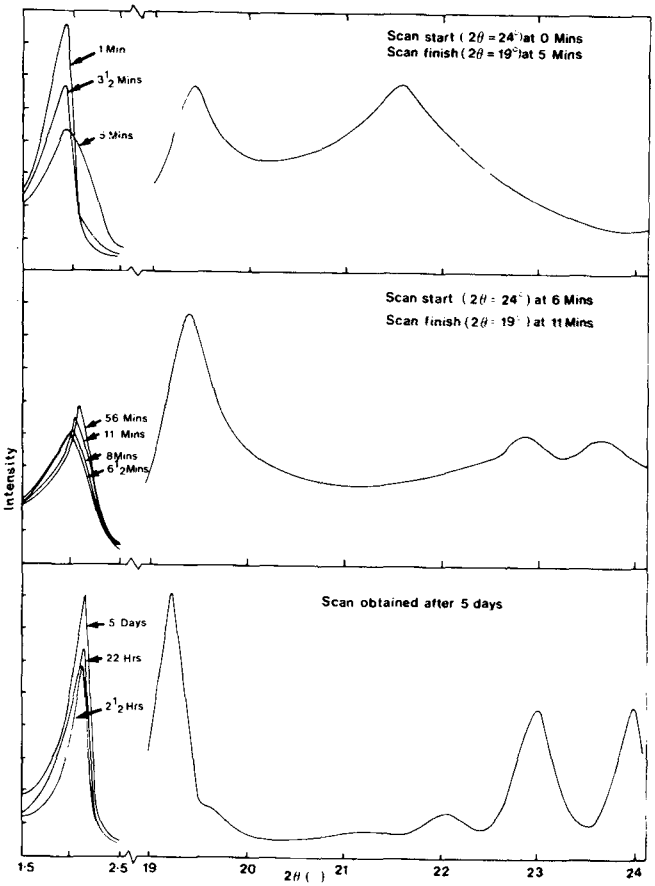

FIG. 8. Typical time dependence of the X-ray diffraction peaks, obtained for a 70% tripalmitin, 30% triolein mixture, after rapid cooling to 277K. The short time studies for the wide and low angle regions were carried out on repeated experiments as the wide angle range takes ∿5 min to scan. Repeats were found to be highly reproducible. The wide angle region shows that 'β-like' crystals are obtained after only a few minutes, but the peaks remain broader than for the long time study. (Comparison of the middle and lower curves.) In order to demonstrate the slowness of the shift in the long d-spacing and to demonstrate the total possible change, the sample was allowed to warm to 298K for the scans shown in the lower curves. The times at which each peak was obtained are shown.

there is little difference in the enthalpy changes, the rapid cooling gives $\Delta H_f = 205 \pm 2\ Jg^{-1}$, and the slow cooling sample $\Delta H_f = 201 \pm 1\ Jg^{-1}$. The different shape suggests that the solubility of the saturated triglyceride is lower in the rapid cooled system. This could be due to the smaller crystals present in the rapid cooled sample which will have a greater total surface area for a set mole fraction of material so giving a greater driving force to demix.

Isothermal changes. A study of the time effects in these mixtures was carried out after rapid cooling. X-ray measurements were made on cooling to different temperatures within the range 270-290K; a time profile of the diffraction peaks obtained at 288K is shown in Figure 8. This demonstrates that two processes occur; the first is complete in a few minutes, as shown by the decrease in intensity and broadening of the peak at $2\theta = 1.8°$. Over the same timescale (1-11 min) in the wide angle range the α diffraction pattern has changed to give the β like spectrum with an absence of a diffraction peak at 21.5°. This shows that little or no α type crystals remain after a few minutes. As seen from the small angle measurements, the long d-spacing is still similar to that of the α-form throughout the first few minutes after rapid cooling.

The wide angle results suggest that within a few minutes the molecules within the crystal are tilted in a way similar to that observed for the β polymorphic form, while the small angle results indicate that the chain packing is staggered to give a distance between crystal layers similar to that observed for the α polymorph. We interpret the angular shift and sharpening of the diffraction peaks over the next few days as the molecules take up a position of maximum overlap and the lowest free energy.

A DSC study showed that, although there was a slight shift toward the slow cooled heat capacity curve over this timescale, it was very small and even the heat capacity at low temperatures remained virtually unchanged.

These results show that at least two processes are occurring, the first being repacking of crystal layers recorded by the X-ray technique and a longer Ostwald ripening process (observed by microscopy for our samples) which is probably the dominant feature in determining the heat capacity of the system.

ACKNOWLEDGMENT

P. J. Lillford and A. H. Clark provided helpful advice and discussion.

REFERENCES

1. Clarkson, C.E., and T. Malkin, J. Chem. Soc. 666 (1934).
2. Larsson, K., Chem. Scr. 1:21 (1971).
3. Dafler, J.R., JAOCS 54:249 (1977).
4. Hvolby, A., JAOCS 51:50 (1974).
5. Lutton, E.S., and A.J. Fehl, Lipids 5:90 (1970).
6. Larsson, K., Ark Kemi 23:1 (1965).
7. Hagemann, J.W., W.H. Tallent and K.E. Kolb, JAOCS 49:118 (1972).
8. Hagemann, J.W., and J.A. Rothfus, JAOCS 60:1123 (1983).
9. Hale, J.E., and F. Schroeder, Lipids 16:805 (1981).
10. Lutton, E.S., JAOCS 32:49 (1955).
11. Hannewijk, J., Chemisch. Weekblad 60:309 (1964).
12. Privalov, P.L., Pure & Appl. Chem. 52:479 (1980).
13. Hampson, F.W., and H.L. Rothbat, JAOCS 46:143 (1969).
14. Charbonnet, G.H., and W.S. Singleton, JAOCS 24:140 (1947).
15. Pines, A., M.C. Gibby and J.S. Waugh, J. Chem. Phys. 59:569 (1973).
16. Schaefer, J., and E.O. Stejskal, JACS 98:1031 (1976).
17. Rossell, J.B., Advan. Lipid Res. 5:353 (1967).
18. Chapman, D., The Structure of Lipids, Methuem & Co. Ltd., London, 1965, pp. 262-280.
19. Pfeffer, P.E., F.E. Luddy, J. Unruh and J.N. Shoolery, JAOCS 54:380 (1977).
20. Farrar, T.C., and E.D. Becker, Pulse and Fourier Transform NMR, Acad. Press, New York, NY, 1971, p. 20.
21. O'Neill, M.J., Analytical Chem. 36:1238 (1964).
22. Kawamura, K., JAOCS 56:753 (1979).
23. Yoncoskie, R.A., JAOCS 44:446 (1967).
24. Hoerr, C.W., and F.R. Paulicka, JAOCS 45:793 (1968).
25. Hartman, S.R., and E.L. Hahn, Phys. Rev. 128:2042 (1962).
26. Haw, J.F., and G.E. Macier, Anal. Chem. 55:1262 (1983).

[Received October 29, 1984]